

# Curvature effects in charge-regulated lipid bilayers

Petch Khunpetch<sup>1,\*</sup>, Arghya Majee<sup>2,3,\*</sup> and Rudolf Podgornik<sup>4,5,6</sup>

<sup>1</sup>*School of Physical Sciences, University of Chinese Academy of Sciences, Beijing, China*

<sup>2</sup>*Max Planck Institute for Intelligent Systems, Stuttgart, Germany*

<sup>3</sup>*IV. Institute for Theoretical Physics, University of Stuttgart, Germany*

<sup>4</sup>*Kavli Institute for Theoretical Sciences,*

*University of Chinese Academy of Sciences, Beijing,*

*China & CAS Key Laboratory of Soft Matter Physics,*

*Institute of Physics, Chinese Academy of Sciences, Beijing, China*

<sup>5</sup>*Wenzhou Institute of the University of Chinese Academy of Sciences, Wenzhou, Zhejiang, China*

<sup>6</sup>*Department of Theoretical Physics, Jožef Stefan Institute,*

*Ljubljana, Slovenia & Department of Physics,*

*Faculty of Mathematics and Physics, University of Ljubljana, Ljubljana, Slovenia*

(Dated: January 17, 2022)

## Abstract

We formulate a theory of electrostatic interactions in lipid bilayer membranes where both monolayer leaflets contain dissociable moieties that are subject to charge regulation. We specifically investigate the coupling between membrane curvature and charge regulation of a lipid bilayer vesicle using both the linear Debye-Hückel (DH) and the non-linear Poisson-Boltzmann (PB) theory. We find that charge regulation of an otherwise symmetric bilayer membrane can induce *charge symmetry breaking*, *non-linear flexoelectricity* and *anomalous curvature dependence of free energy*. The pH effects investigated go beyond the paradigm of electrostatic renormalization of the mechano-elastic properties of membranes.

---

\* Equal contribution and shared co-first authorship

## I. INTRODUCTION

The effects of electrostatic interactions [1, 2] on properties of lipid bilayer membranes are significant, ubiquitous and biologically [3] and biomedically [4] relevant, since naturally occurring as well as technologically relevant lipids usually carry numerous dissociable or polar groups [5], and lipid membrane charge density has been identified as a universal parameter that quantifies the transfection efficiency of lamellar cationic lipid–DNA complexes [4]. The particular relevance of electrostatic interactions in lipidic systems very clearly transpired from the structural principles of the two vaccines approved against COVID-19 in December 2020 and based on the cationic lipid vesicle vector and the anionic mRNA payload developed by Pfizer/BioNTech [6] and Moderna [7]. In general, ionizable lipids, capable of modulating their charge depending on the bathing environmental conditions, have been recognized as a key component of *ionizable lipid nanoparticles* which are currently acknowledged as one of the most advanced non-viral vectors for the efficient delivery of nucleic acids [8].

While electrostatic interactions in bio-soft matter are universal [9], there is a fundamental difference between the standard colloid electrostatics and membrane electrostatics [10], in the sense that the membrane charge, just as the protein charge [11–13], depends on the solution environment of the lipid [14] and its changes can engender also changes in the shape of the lipids and concomitant structure of lipid assemblies. One example of this solution environment effect would be changes in protonation/deprotonation equilibria of the dissociable phospholipid moieties depending on the solution pH, that in general affect the charge of lipids' headgroup, and another would be the modification of the strength of electrostatic interactions wrought by the ionic strength of the bathing aqueous solution that affects the ionic screening. In particular, for therapeutic gene delivery [15] ionizable lipids are designed to have positive charges at acidic pH in the production stage to ensure a strong interaction with nucleic acids, after which they should become almost neutral under physiological conditions (pH 7.4) to prevent sequestration in the liver, and should finally turn positive again upon being introduced into a typical acidic environment of the endosomes, promoting the delivery of the genetic cargo, followed finally by release of the genetic cargo at neutral pH would enabling the cargo to interact with the cell machinery [8].

To connect the dissociation equilibria of dissociable surface groups and electrostatic fields, Ninham and Parsegian (NP) [16] introduced the charge regulation (CR) mechanism, that couples the Langmuir isotherm model of the local charge association/dissociation process with the local electrostatic potential [1], resulting in a self-consistent boundary electrostatic condition. The NP model can be generalized to include other adsorption isotherm, depending on the detailed nature of the dissociation process [17].

The protonation/deprotonation equilibria at the dissociable surface groups in phospholipid membranes involve local pH and local bathing solution ion concentrations, which in general differ from the bulk conditions [18]. This implies that the changes in the bathing solution properties will have a pronounced effect on the effective charge of the membrane, thus modifying pH sensing and pH response of lipid membranes [19]. In fact, pH-dependence of the lipid charging state can directly enable an ionizable lipid with a  $pK_a$  around 6.5 to be neutral in the blood circulation, thus preserving a bilayer structure, and then revert to its charged protonated form at an endo-lysosomal pH, consequently reverting to an hexagonal phase upon contact with anionic membrane lipids [20].

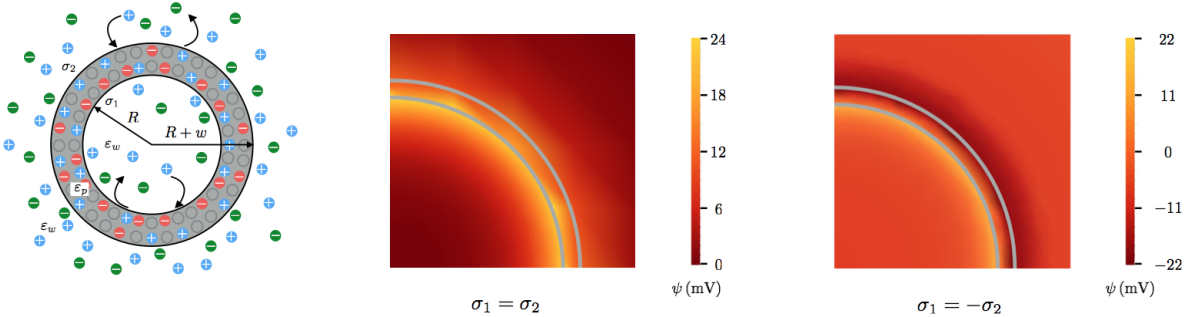


FIG. 1. Left: A schematic rendition of a spherical charged vesicle of inner and outer radii  $R$  and  $R + w$ , respectively, immersed in a salt solution. The lipid bilayer (indicated in gray) of width  $w$  and dielectric constant  $\epsilon_p \approx 5$  separates the interior of the shell from the outer region, both of which are typically aqueous phases characterized by a dielectric constant  $\epsilon_w \approx 80$ . All the ionic species in both regions are assumed to be in chemical equilibrium defined by the bulk chemical potentials. Both the inner and outer surfaces of the bilayer carry fixed numbers of negatively charged surface groups (denoted in red) as well as neutral sites where (de)protonation reactions (indicated by the arrows) can take place leading to surface charge densities  $\sigma_1$  and  $\sigma_2$ . Center and right: the color-coded electrostatic potential profile for the symmetric case, corresponding to  $\sigma_1 = \sigma_2 = 0.5 \text{ e/nm}^2$  and for the asymmetric case with  $\sigma_1 = -\sigma_2 = 0.5 \text{ e/nm}^2$  obtained from the charge regulation calculation as explained in the main text. For both cases,  $R = 20 \text{ nm}$ ,  $w = 1 \text{ nm}$ , and  $\kappa_D = 1.22 \text{ nm}^{-1}$  are used.

In what follows we will show that even in the case of a chemically symmetric curved membrane, *i.e.* with the same lipid composition on the inner and outer leaflets, the CR process introduces a charge asymmetry and a membrane polarization vector in a highly non-linear fashion, characterized by a sudden symmetry breaking transition involving in all other respects *chemically identical* outer and inner leaflet surfaces of the membrane. This phenomenology closely parallels the recently discovered symmetry breaking charge transitions in interactions between pairs [21] or stacks [22] of charged membranes as well as the complex coacervation driven by the charge symmetry broken states in solutions of macroions with dissociable surface moieties [23].

**Charged lipids.** Different naturally occurring charged lipid species, an important fraction of which is anionic [24], represent a notable part of biological membranes, and consequently their role in the structural, dynamical and mechanical properties of model lipid bilayers as well as their effect on the membrane proteins is of great biological interest [25]. The less commonly occurring cationic lipids, on the other hand, have played an important role as the main charged component of the cationic liposome vectors for nucleic acid therapeutics [15].

The charge of phospholipid polar heads originates in deprotonated phosphate groups, protonated amine group, and deprotonated carboxylate group, with the corresponding dissociation constants expected to lie in the region of  $0 \leq pK_a \leq 2$  for the primary phosphate group, in the region  $6 \leq pK_a \leq 7$  for the secondary phosphate group, in the region  $3 \leq pK_a \leq 5$  for the carboxylate groups, and  $9 \leq pK_a \leq 11$  for the primary amine group [26]. Since in the subsequent analysis the effect of the electrostatic interactions - including the local polarity, the ionic strength and the distribution of neighboring dissociable groups - will be considered explicitly, we consider only the

intrinsic  $pK_a$ , noting that even in the absence of CR certain structural and continuum electrostatic effects are sometimes included in the calculation of the dissociation constants when determined by e.g. PROPKA [27].

Of the different phospholipids, phosphatidylcholines have very low  $pK_a$  and can be considered as undissociated, but in particular phosphatidylserine, phosphatidylinositol, as well as phosphatidylglycerol, phosphatidylethanolamine, cardiolipin and phosphatidic acid all contain at least one dissociable moiety at relevant pH conditions and should be considered as potentially charged [28]. Among the cationic lipids DOTAP (1,2-dioleoyl-3-trimethylammonium-propane) remains charged irrespective of pH, while the amine groups of other cationic lipids acquire their charge by protonation only below a certain pH [29]. As an extreme case one could mention the custom-synthesized cationic lipid MVLBG2 with a headgroup that bears no less than 16 positive charges at full protonation [4]. In ionizable lipids the quaternary ammonium head of cationic lipids can be in addition substituted with a titratable molecular moiety with an engineered dissociation constant that would ensure the charge would be mouldable by the environmental pH [8]. Among the ionizable lipids that respond strongly to pH in the relevant range one can list DODAP (1,2-dioleoyl-3-dimethylammonium propane), DLinDMA, DLin-KC2-DMA and finally DLin-MC3-DMA, all of them used for proper lipid vector formation in cytosolic delivery of therapeutic cargo as reviewed recently in Ref. [8].

*Protonation and pH effects.* Detection and response of the cells to either global pH environment or local pH gradients is crucial for optimal cellular metabolism, growth and proliferation [30]. The sensing of pH heterogeneities is important for initiating migration, polarization and deformations of lipid bilayer assemblies [19] and can be driven by protonation changes of phospholipids that can furthermore directly affect the membrane curvature [31]. In fact pH regulation of phospholipid charges have been implicated in pH-induced migration, pH-induced bilayer local or global deformation, as well as pH-induced vesicle chemical polarization [19]. The fact that the charge state of many phospholipids depends on the solution pH implicates by and large a charge regulation mechanism as indeed first proposed for surfaces containing dissociable groups by Ninham and Parsegian [16].

In addition, the phospholipid protonation state and the membrane charge distribution can modify the interaction energy with a protein on approach to the membrane [32]. This effect too is due to perturbed protonation equilibrium at the membrane titratable sites, with phospholipid charge regulation determining the strength and even the sign of the protein-membrane interaction in variable chemical environments [33]. Charge regulation can thus be seen as a *biological pH-sensitive switch* for protein binding to phospholipid membranes thus conferring signaling functions to different types of lipids [34].

*Curvature and lipid dissociation effects.* Global and local changes in pH, inducing changes in the charged states of lipids, can affect lipid vesicle shape deformations as well as phase-separated domain formation [19]. Usually these effects are framed within the electrostatic contribution to the mechano-elastic properties of membranes, such as surface tension and bending rigidity, which have been reviewed in detail, see e.g. Refs. [35], [36] and [24]. Electrostatic coupling of membrane charges leads to a salt concentration dependent increase in the bending rigidity of the charged membrane compared to a charge-free membrane [37]. Usually the details of lipid dissociation mechanism is not considered in these works and analyses going beyond the fixed

charge assumption, incorporating direct lipid charge dissociation models, are less common but have been nevertheless invoked when modelling the flexoelectric properties of membranes [38]. In fact Langmuir adsorption isotherm was used to estimate the change in the surface density of counterions on the inner and outer leaflet surface of the phospholipid membrane induced by the coupling between curvature and electrostatics [39].

In what follows we will present a detailed analysis of the charge regulation effects in a system, see Fig. 1, comprised of a single spherical unilamellar lipid vesicle of a fixed phospholipid membrane thickness  $w \simeq 1$  nm, dielectric constant  $\epsilon_p \simeq 5$  and variable radius  $R$ , immersed in a simple univalent electrolyte solution, of dielectric constant  $\epsilon_w \simeq 80$ . We will use the full Poisson-Boltzmann (PB) theory to evaluate the electrostatic part of the free energy, as well as the often invoked and easier to implement linearized Debye-Hückel (DH) theory in the second order curvature expansion approximation. This will allow us to ascertain which effects are non-linear in nature as far as electrostatics is concerned. We will show that charge regulation of an otherwise symmetric bilayer membrane induces three important phenomena: *charge symmetry breaking, non-linear flexoelectricity and anomalous curvature dependence of free energy* and that in general the pH effects go beyond the paradigm of electrostatic renormalization of the mechano-elastic properties of membranes.

The outline of the paper is as follows: In Sec. II, we describe the details of the charge regulation model and formalism for this study. Section III is devoted for the results of the study. Finally, the discussion of the results of the curvature effects in charge-regulated lipid bilayers is given in Sec. IV.

## II. MODEL AND FORMALISM

### A. Model

The description of charge regulation is model specific and there is no universal model that would be applicable to any situation encountered in biophysical systems. We base our model on the preponderance of three different types of interactions that can be deemed as important in the context of ionizable lipids: (i) electrostatic interactions, (ii) non-electrostatic adsorption interactions and (iii) adsorption site entropy.

We consider a spherically charged vesicle with a salt solution on the two sides of its bilayer membrane as shown in Fig. 1. The inner radius of the charged shell is  $R$  with charge density  $\sigma_1$  and the outer radius is  $R+w$  with charge density  $\sigma_2$ . The lipid bilayer composes of two charge-regulated monolayers. We assume that  $n_{1,2}$  is the number of negative lipid heads per surface area of the inner and outer monolayers, respectively, and  $\Theta n_{1,2}$  is the number of neutral lipid heads per surface area of the inner and outer monolayers, respectively. Furthermore,  $\eta_{1,2}$  are the fractions of the neutral lipid heads where the adsorption/desorption of cations can take place on the inner and outer monolayers, respectively. By definition,  $\eta_{1,2} \in [0, 1]$ .  $e$  is the elementary charge ( $e > 0$ ). Here, we have modified the model discussed in [21]. The connection between lipid density, charge density and adsorbed fraction is as follows:

$$\sigma_i = -n_i e + \Theta n_i e \eta_i. \quad (1)$$

In our model,  $\sigma_{1,2}$  and  $\eta_{1,2}$  are assumed to be uniform over the two monolayers and we consider the case  $\Theta = 2$  for simplicity. This assumption reduces Eq. (1) to

$$\sigma_i = 2n_i e \left( \eta_i - \frac{1}{2} \right), \quad (2)$$

with  $-en_{1,2} \leq \sigma_{1,2} \leq en_{1,2}$ . Other choices of  $\Theta$  are of course also possible depending on the exact composition of the bilayer. This does not, however, impact the qualitative features of our results. The static dielectric constant of water is assumed as  $\varepsilon_w = 80$  and that of the lipid bilayer membrane as  $\varepsilon_p = 5$ . The Debye screening length ( $\lambda_D$ ) varies from about 0.34 nm to 10.75 nm corresponding to the monovalent salt concentration ranging from 1 – 0.001M [40]. Moreover, we define  $\mu = \varepsilon_p / \varepsilon_w$ .

Charge regulation can be quantified either through the chemical equilibrium of dissociable sites at the bounding surface or through the surface free energy if the interactions between the solution charges and the surface is characterized by short-range ion-specific interactions [17]. The latter seems more appropriate within the context of mean-field electrostatics.

In general, charge regulation is related to any non-trivial, *i.e.* non-zero, form of the surface free energy describing different models of surface-ion solution interactions [10]. The single site dissociation model can be related to van't Hoff adsorption isotherm, Langmuir (Henderson-Hasselbalch) adsorption isotherm, Frumkin-Fowler-Guggenheim adsorption isotherm and others [17]. Following the analysis of charged surfactant systems [41] we base our phospholipid charge regulation model on the Frumkin-Fowler-Guggenheim isotherm [42] defined with the phenomenological free energy of a single adsorption site in the units of thermal energy  $k_B T = 1/\beta$  as

$$\beta \mathcal{F}_{CR} [\eta] = \oint_A dA \left[ -\alpha \eta(\rho) - \frac{1}{2} \chi \eta(\rho)^2 + \eta(\rho) \ln(\eta(\rho)) + (1 - \eta(\rho)) \ln(1 - \eta(\rho)) \right], \quad (3)$$

where the integral is over the surface with dissociable groups and  $\rho$  is the radius vector on this surface. For a spherical surface of radius  $R$ ,  $|\rho| = R$ .

The parameters  $\alpha$  and  $\chi$  in the above definition are phenomenological and describe the non-electrostatic part of the proton-macroion and the proton-proton interactions at the macroion surface expressed in the units of the thermal energy. A more general, non-local version of the latter would be,

$$\oint_A dA \frac{1}{2} \chi \eta(\rho)^2 \rightarrow \oint_A dA dA' \frac{1}{2} \chi(\rho - \rho') \eta(\rho) \eta(\rho'), \quad (4)$$

which, however, we will not pursue in what follows, limiting ourselves to the simplified Frumkin-Fowler-Guggenheim isotherm of Eq. (3).

In the case of (de)protonation reaction, the dependence of  $\alpha$  on the bulk pH is model specific [14], but can be written as a sum of

$$\alpha = \Delta g + \mu = \Delta g + k_B T \log [H^+], \quad (5)$$

on the PB mean-field level, where  $\Delta g$  is the dissociation free energy difference and  $\mu = k_B T \log [H^+]$  is the chemical potential of the dissociation product, in our case the protons. Consequently, on the mean-field level one can express  $\Delta g$  via the dissociation equilibrium constant and  $[H^+]$  via the pH, in order to explicitly identify  $\alpha = (pK_a - \text{pH}) \ln 10$ , where  $\text{pH} = -\log_{10}[H^+]$ , with  $[H^+]$  being the

proton concentration in the bulk and  $pK_a$  the dissociation constant of the deprotonation reaction, in the case of the Langmuir adsorption model [16], which is equivalent to a Henderson-Hasselbalch equation with electrostatics included [43]. Furthermore,  $\chi$ , as in the related lattice regular solutions theories (e.g., the Flory-Huggins theory [44]) describes the short-range interactions between nearest neighbor adsorption sites on the macroion surface [45]. A parameter value  $\alpha \leq 0$  encodes a favorable adsorption free energy between protons and the macroion surface, while  $\chi \geq 0$  represents the tendency of protons on the macroion surface adsorption sites to phase separate into domains.

Adding also the electrostatic energy, as will be done in the next section, our model will therefore incorporate all three fundamental interactions: electrostatic interactions, non-electrostatic interactions between the lipids and the solution ions as well as non-electrostatic interactions between the adsorbed ions, and the adsorption site entropy.

## B. Electrostatic free energy

We start with the standard Poisson-Boltzmann free energy, or the Debye-Hückel free energy in the linearized case, that depends on the charges and the curvature. There are various ways to write down the PB free energy [1] and we choose the field description, with the radially varying electrostatic potential  $\psi(r)$  as the only relevant variable. The total electrostatic free energy of our model system is then

$$\mathcal{F}_{ES} = - \int dV \left[ \frac{1}{2} \varepsilon_w \varepsilon_0 \left( \frac{d\psi(r)}{dr} \right)^2 + 2n_I (\cosh \beta e \psi(r) - 1) \right] + \oint_{A_1} dA_1 \psi(R_1) \sigma_1 + \oint_{A_2} dA_2 \psi(R_2) \sigma_2, \quad (6)$$

where  $n_I$  is the uni-univalent electrolyte concentration in the bulk,  $R_1 = R$  and  $R_2 = R + w$ , with  $w$  the thickness of the membrane, while the equilibrium value of  $\psi(r)$  is obtained from the corresponding Euler-Lagrange equation. The volume integral extends over all the regions except the bilayer interior. The electrostatic part of the thermodynamic potential can then be written with the help of the *Casimir charging formula* (for details see Ref. [46]) which allows one to write the full thermodynamic potential of the system in the form of a surface integral

$$\mathcal{F}_{ES}(\sigma_1, \sigma_2, R) = \sum_{i=1}^2 4\pi R_i^2 \int_0^{\sigma_i} d\sigma_i \psi(R_i, \sigma_i), \quad (7)$$

where  $i = 1, 2$  corresponds to inner/outer leaflets of the bilayer. In the above equation note the integral of the boundary potential over the surface charge densities, pertinent to the full non-linear PB theory. From here it also clearly follows that

$$\frac{\partial \mathcal{F}_{ES}(\sigma_1, \sigma_2)}{\partial \sigma_i} = 4\pi R_i^2 \psi(R_i), \quad (8)$$

which we will invoke in the mean-field form of the charge regulation boundary conditions, to be introduced later.

A common approach to electrostatic effects in membranes is via the DH approximation together with small curvature, second order expansion [24, 35, 36]. In the DH approximation, valid

specifically for  $\beta e\psi(r) \ll 1$ , the corresponding expressions for the electrostatic free energy Eq. (6) simplifies considerably to

$$\mathcal{F}_{ES} = -\frac{1}{2}\epsilon_w\epsilon_0 \int dV \left( \left( \frac{d\psi(r)}{dr} \right)^2 + \kappa_D^2 \psi(r)^2 \right) + \oint_{A_1} dA_1 \psi(R_1) \sigma_1 + \oint_{A_2} dA_2 \psi(R_2) \sigma_2, \quad (9)$$

where the inverse square of the Debye screening length  $\lambda_D$  is given by  $\kappa_D^2 = 2n_I\beta e^2/\epsilon_w\epsilon_0$  and the volume integral again extends over all the regions except the bilayer interior. Eq. (9) is then further reduced to

$$\mathcal{F}_{ES}(\sigma_1, \sigma_2, R) = 2\pi \sum_{i=1}^2 R_i^2 \sigma_i \psi(R_i, \sigma_i), \quad (10)$$

since the potentials are linear functions of the charge density and the integrals over surface charge densities in the Casimir formula can be evaluated explicitly. Within the phospholipid core of the bilayer the electrostatic energy is simply

$$\mathcal{F}_{ES} = -\frac{1}{2}\epsilon_p\epsilon_0 \int dV \left( \frac{d\psi(r)}{dr} \right)^2 + \oint_{A_1} dA_1 \psi(R_1) \sigma_1 + \oint_{A_2} dA_2 \psi(R_2) \sigma_2, \quad (11)$$

where the volume integral now extends over the bilayer interior. While the free energies Eq. (6) and Eq. (9) imply the PB and the DH equation in the regions accessible to electrolyte ions [47], respectively, Eq. (11) leads to the standard Laplace equation inside the lipid dielectric core.

The explicit DH expression for the electrostatic free energy per area was obtained as a function of the radius of curvature  $R$  to inverse quadratic order in Ref. [40] and is rewritten in terms of Eq. (2) in the Appendix (see Eq. (A2)).

The DH electrostatic free energy displays a general quadratic dependence on the curvature of the lipid bilayer. This quadratic dependence of electrostatic free energy was standardly taken as a point of departure for the electrostatic renormalization of the mechanical properties of membranes, such as surface tension and bending rigidity [48–52].

### C. Charge regulation free energy

Assuming that the inner and outer membrane surfaces are chemically identical we presume that the surface charge regulation process can be described by the Frumkin-Fowler-Guggenheim adsorption isotherm, including the adsorption energy, the interaction energy between adsorbed species and the site entropy.

The corresponding free energy is then given by Eq. (3) so that the charge regulation free energy density of the inner and outer membrane surfaces denoted by  $i = 1, 2$  read as

$$\frac{\mathcal{F}_{CR}(\eta_i)}{4\pi R_i^2} = n_{i0}k_B T \left[ -\alpha\eta_i - \frac{\chi}{2}\eta_i^2 + \eta_i \ln \eta_i + (1 - \eta_i) \ln(1 - \eta_i) \right], \quad (12)$$

This can be furthermore normalized w.r.t. the inner area  $4\pi R^2$  which is used later. The first two terms in the free energy are enthalpic in origin. The other terms are the mixing entropy of charged sites with the surface area fraction  $\eta$  and neutralized sites with the surface area fraction  $1 - \eta$ .

It is important to reiterate at this point that other charge regulation models are of course possible [17] and have been proposed for various dissociable groups in different contexts [10]. Our reasoning in choosing the particular Frumkin-Fowler-Guggenheim isotherm was guided by its simplicity in the way it takes into account the salient features of the dissociation process on the membrane surface, and the fact that the implied phenomenology has been analyzed before in the context of charged soft matter systems [41].

#### D. Curvature - lipid density coupling free energy

Apart from the electrostatic energy and the charging energy one needs to consider also the pure lipid bilayer elastic energy, extensively reviewed within different conceptual backgrounds [53–55].

In order to introduce a minimal amount of additional parameters, we assume that for a deformed bilayer the lipid density at the outer (2) and inner (1) monolayer surface projected onto the midsurface of the bilayer is modified because of the curvature. The stretching and curvature elastic energies of the bilayer can then be cast as [56, 57]:

$$\mathcal{F}_{HE}(n_1, n_2; H) = \oint_{(A)} dA \left[ \frac{k_s}{2} \left( \frac{n_1 - n_{10}}{n_{10}} - wH \right)^2 + \frac{k_s}{2} \left( \frac{n_2 - n_{20}}{n_{20}} + wH \right)^2 + \frac{k_b}{2} H^2 \right], \quad (13)$$

where the integral is over the bilayer midplane, and

$$H = (c_1 + c_2) = \frac{2}{\left( R + \frac{w}{2} \right)} \quad (14)$$

is the mean curvature of the midplane of the bilayer with  $c_1$  and  $c_2$  being the principal curvatures,  $k_s$  and  $k_b$  are the elastic compression modulus and the bending modulus, respectively, and  $w$  is the thickness of the bilayer.  $n_{10,20}$  are the reference densities of the lipids in the two flat monolayers, while  $n_{1,2}$  are the lipid densities of the curved monolayers projected onto the midsurface of the bilayer. We have also assumed that the monolayers are symmetric and have no intrinsic spontaneous curvature.

The above free energy contribution obviously couples the lipid density in the two constitutive monolayers with the curvature of the bilayer. Assuming a constant curvature of the bilayer midplane (see Fig. 1), this coupling free energy density can be rewritten equivalently also as

$$\frac{\mathcal{F}_{HE}(n_1, n_2; R)}{4\pi R^2} = \left( 1 + \frac{w}{2R} \right)^2 \left[ \frac{k_s}{2} \left( \frac{n_1}{n_0} - 1 - \frac{2w}{R + \frac{w}{2}} \right)^2 + \frac{k_s}{2} \left( \frac{n_2}{n_0} - 1 + \frac{2w}{R + \frac{w}{2}} \right)^2 + \frac{2k_b}{\left( R + \frac{w}{2} \right)^2} \right], \quad (15)$$

where we have furthermore assumed that the membrane is chemically symmetric, i.e.,  $n_{10} = n_{20} = n_0 = a^{-2}$  with  $a \simeq 1$  nm. For a typical system one has  $k_s \simeq 10^2 k_B T / \text{nm}^2$ ,  $k_b \simeq 10 k_B T$  and  $w \simeq 4$  nm.

#### E. The total free energy density

Combining now the electrostatic free energy, the charge regulation free energy and the curvature - lipid density coupling free energy, i.e., combining Eq. (A2) of the Appendix (rewritten in terms of

Eq. (2)) within the DH theory or Eq. (6) within the PB theory with Eqs. (11), (12), and (15), we are led to the explicit form of the total free energy of our model system (Eq. (A3) in the Appendix) as

$$\frac{\mathcal{F}_{tot}(n_1, n_2; \eta_1, \eta_2; h)}{4\pi R^2} = \frac{\mathcal{F}_{ES}(n_1, n_2; \eta_1, \eta_2; h)}{4\pi R^2} + \frac{\mathcal{F}_{HE}(n_1, n_2; h)}{4\pi R^2} + \frac{\mathcal{F}_{CR}(\eta_1; h) + \mathcal{F}_{CR}(\eta_2; h)}{4\pi R^2}. \quad (16)$$

Here we have defined the dimensionless curvature

$$h \equiv 1/(\kappa_D R) \quad (17)$$

which will feature as one of the main variables in our analysis. In order to find the equilibrium state of the system, the total free energy Eq. (16) needs to be minimized with respect to the four variables  $\eta_{1,2}$  and  $n_{1,2}$ . This turns out to be a tedious exercise as the final system of equations is non-linear and is even numerically quite complicated to solve. We thus take recourse to an additional simplification that will eliminate two of these variables by considering the bilayer as basically unstretchable.

#### F. Limit of unstretchable bilayer

Since minimization with respect to all four variables in Eq. (16) is difficult and prone to numerical problems, we resort to a limiting case of a vanishing elastic compression, which yields a relationship between the projected lipid density, the reference density and the bilayer curvature of

$$n_i = n_{i0} (1 \pm wH). \quad (18)$$

In this way the two coupling terms in Eq. (15) vanish. We furthermore assume that the two monolayers are chemically identical, *viz.*  $n_{10} = n_{20} = n_0$ . Clearly the effective density of the lipids is increased on the inner leaflet and is decreased on the outer leaflet in proportion to the curvature of the bilayer.

This limit furthermore implies that the charge densities in Eq. (2) are:

$$\sigma_i = 2n_0e (1 \pm wH) \left( \eta_i - \frac{1}{2} \right), \quad (19)$$

where + and – occurring for  $i = 1$  and 2, respectively. The electrostatic free energy then becomes

$$\frac{\mathcal{F}_{ES}(n_1, n_2; \eta_1, \eta_2)}{4\pi R^2} \longrightarrow \frac{\mathcal{F}_{ES}(\eta_1, \eta_2)}{4\pi R^2}. \quad (20)$$

Clearly this reduces the number of variables to two:  $\eta_1$  and  $\eta_2$ , making it a manageable calculation. The corresponding free energy is then obtained in the form

$$\frac{\mathcal{F}_{tot}(\eta_1, \eta_2; h)}{4\pi R^2} = \frac{\mathcal{F}_{ES}(\eta_1, \eta_2; h)}{4\pi R^2} + \frac{2k_b}{R^2} + \frac{\mathcal{F}_{CR}(\eta_1; h) + \mathcal{F}_{CR}(\eta_2; h)}{4\pi R^2}, \quad (21)$$

which is given explicitly in the Appendix (Eq. (B1)). Nevertheless even in this simplified form we can only minimize this free energy numerically as the charge regulation part contains non-linear terms. We proceed in steps.

### G. Charge regulation boundary condition

The thermodynamic equilibrium is now obtained by minimizing the free energy Eq. (21). We get two equations that correspond to charge regulation boundary conditions

$$\frac{\partial \mathcal{F}_{ES}(\sigma_1, \sigma_2)}{\partial \sigma_i} \frac{\partial \sigma_i}{\partial \eta_i} + \frac{\partial \mathcal{F}_{CR}(\eta_i)}{\partial \eta_i} = 0. \quad (22)$$

By taking into account Eqs. (2) and (8), as well as the form of the charge regulation free energy Eq. (12) we derive the dissociation isotherm as

$$2\beta e\psi(R_i)(1 \pm wH) = \alpha + \chi\eta_i - \ln\left(\frac{\eta_i}{1 - \eta_i}\right), \quad (23)$$

with + and – being used for  $i = 1$  and  $2$ , respectively. In the limit of a vanishing curvature the above boundary condition thus corresponds to the Frumkin-Fowler-Guggenheim adsorption isotherm [17, 42] which is often invoked as a model in charge regulation problems [21, 22, 45, 58].

The boundary condition derived above, together with the solution of either full PB equation or the linearized DH version for the electrostatic potential constitute the basic equations of our model, the solutions of which we address next.

## III. RESULTS

For all the numerical evaluation presented herein, we have used typical system parameters such as an inverse Debye length  $\kappa_D = 1.215 \text{ nm}^{-1}$ , or equivalently, screening length  $\lambda_D = 0.823 \text{ nm}$  corresponding to an aqueous electrolyte solution with salt concentration  $n_I = 140 \text{ mM}$ , the Bjerrum length  $\ell_B = 0.74 \text{ nm}$ ,  $\mu = 5/80$ ,  $n_0 = 1 \text{ nm}^{-2}$ , and  $w = 4 \text{ nm}$ . However, the curvature  $h$  and the two interaction parameters  $\alpha$  and  $\chi$  are varied within relevant ranges and their effect on the charge densities of the two lipid monolayers are extensively studied. In addition, we also present the differences between the full non-linear PB theory and the linearized DH theory, which is often used to quantify the electrostatic effects in membranes [55]. Clearly both calculations exhibit similar qualitative features, but can be quantitatively quite different. We scan the parameter space in order to identify the important phenomena connected with charge regulation, which is our primary focus here, but do not specifically apply our model to any particular lipid membrane system.

From our previous works [21, 22] on two CR surfaces interacting across an electrolyte solution we know that depending upon the values of the parameters  $\alpha$  and  $\chi$  the Frumkin-Fowler-Guggenheim adsorption isotherm can lead to a charge symmetry breaking transition, corresponding to unequal equilibrium charge of two surfaces. Here we note that  $\alpha = (pK_a - \text{pH}) \ln 10$  quantifies the pH effects as compared to the dissociation constant of the deprotonation reaction, while  $\chi$  quantifies non-electrostatic interactions between the dissociated sites on the membrane. The charge asymmetry was found to be highest around the line  $\chi = -2\alpha$  and the charge symmetry broken region persisted also in the neighborhood of this line in the earlier works [21, 22]. The present case, however, differs from the model in Ref. [21] in the sense that the region between the two charged phospholipid leaflets is a dielectric, impermeable to electrolyte ions, while the electrolyte solution fills the rest of the space, and thus the salient features of the charging behavior show a rather different behavior.

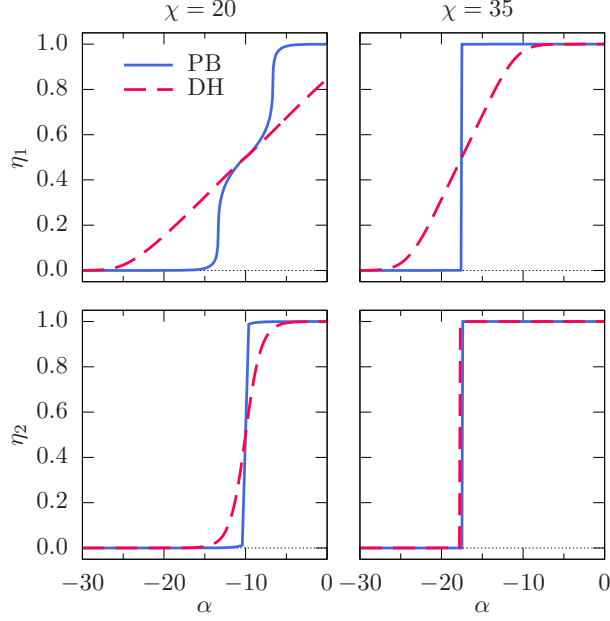


FIG. 2.  $\eta_{1,2}$  as function of  $\alpha$  at two different values of the  $\chi$ -parameter for  $h = 0.02$ . As one can infer from the plots, the discontinuous transition in at least one of the  $\eta_{1,2}$  starts to show up at a smaller  $\chi$ -value within PB theory compared to that within the DH theory. In addition, the results also show symmetry-broken states ( $\eta_1 \neq \eta_2$ ) for  $\chi = 20$  within the PB theory and for both choices of the  $\chi$ -parameter within the DH theory.

In fact while in our system we still find a symmetry breaking transition in the charging fractions,  $\eta_{1,2}$ , the symmetry broken charge region and the symmetric charge regions occupy switched places in the  $(\alpha, \chi)$  "phase diagram" if compared to the case of Ref. [21]; the line  $\chi = -2\alpha$  and its neighborhood thus corresponds to the symmetric charge region, while the rest of the "phase diagram" is symmetry broken. In addition, the extent of the symmetric region also depends on the curvature of the membrane,  $h$ , in such a way that the larger the curvature the larger is the extent of the charge symmetry broken region. This trend starts already at very small values of curvature. We now elucidate these statements in all the relevant detail.

The two charge fractions  $\eta_{1,2}$  as a function of  $\alpha$  are displayed for different  $\chi$  and a fixed membrane curvature  $h$  in Fig. 2. Clearly, for  $\chi = 20$  even at the small curvature  $h = 0.02$  (corresponding to  $R = 41.15$  nm), both the PB and DH results show a pronounced charge asymmetry, which becomes even more prominent for higher values of  $h$ , see Fig. 3 for details. This charge asymmetry corresponds to the *charge symmetry breaking* in the bilayer. In addition, the charge fractions are not only different but can exhibit a discontinuous transition as a function of  $\alpha$ . For  $\chi = 20$  only the PB results show this transition for  $\eta_2$ , whereas the DH results do not; for  $\chi = 35$  the PB results show a discontinuity for both  $\eta_1$  and  $\eta_2$ , while the DH results show a discontinuity only for  $\eta_2$  in the charge state of the lipids. As the curvature is increased the system remains in a charge symmetry broken state between the outer and inner leaflets of the membrane. We therefore conclude that for a spherical vesicle with finite, even if small, curvature the charge regulation standardly leads to a charge symmetry broken state. As a result the values for the charge fractions of the inner and the outer membrane layer differ even if the two leaflets of the lipid membrane are chemically identical. In addition, depending on the values of the charge regulation model parameters and curvature, the

dependence of  $\eta_{1,2}$  on either  $\alpha$  or  $\chi$  can be continuous or discontinuous.

In order to be able to analyze the dependence of the charge densities  $\sigma_1, \sigma_2$  of the two membrane leaflets on the charge regulation parameters, we present a phase diagram in Fig. 3 that shows the variation of  $|\sigma_1 - \sigma_2|$  as a function of  $\alpha \in [-20, 20]$  and  $\chi \in [0, 40]$  for  $h = 0.1, 0.5, 1.0$ , and  $2.0$ . The (white) regions, corresponding to charge symmetric states of the two leaflets, are clearly discerned and their location and extent depends on  $\alpha$  and  $\chi$ , as well as on the bilayer curvature  $h$ , which obviously has a profound effect on the charge state of the bilayer, *i.e.*, on the value of  $|\sigma_1 - \sigma_2|$ . We reiterate that in the previous work [21, 22] the symmetry broken region was centered on the line  $\chi = -2\alpha$ , while in the present case it is the symmetric state which is centered on that line, while the rest of the phase diagram corresponds to a symmetry broken state.

In addition, for  $h = 0.1$ , we actually see not one but three regions of charge symmetric states, corresponding to  $\sigma_1 = \sigma_2$  (indicated by white color in Fig. 3, almost coinciding for both non-linear PB and linear DH calculations. From the phase diagram it is difficult to see what the three symmetric branches correspond to, but we will later show that they correspond to the change in sign of the charge density difference  $\sigma_1 - \sigma_2$ . Among the regions with charge symmetry, the one centered on  $\chi = -2\alpha$  (the middle region) passes through almost the same range of  $\alpha$  for both calculations. At  $h = 0.5$ , the line  $\chi = -2\alpha$  fully passes through the range  $\alpha \in [-20, 0]$  in the DH theory, while in the PB theory, the line is terminated at  $\alpha \approx -16$ . Further increasing the curvature to 1.0 and beyond, the line is terminated at  $\alpha = -20$  for both theories. The more pronounced asymmetric states in Fig. 3 of the PB case extend over a broader region than for the DH case at  $h = 0.1$  and 0.5. With increasing  $h$  up to 1.0 and higher, the phase diagram shows clearly that only the PB case can exhibit the highest asymmetry (represented by dark blue color, while the DH solution remains broadly less asymmetric. Also the PB theory exhibits a wider range of  $|\sigma_1 - \sigma_2|$  values than the DH solution.

We now turn our attention to the details of the curvature dependence of the charge state of the membrane. At the beginning a *caveat* is in order: the very small values of the curvature are only accessible in the DH approximation, whereas the solution of the full PB theory take unreasonably long time because the system size has to be increases concurrently with the decrease in curvature. It is for this reason that the curvature dependence in the PB theory is truncated at finite values of curvature. The curvature dependence of the difference between the inner and outer charge density,  $\sigma_1 - \sigma_2$ , for negative and positive values of  $\alpha$  is fully displayed in Figs. 4 and 5, respectively. Obviously this dependence is fundamentally non-monotonic, including the changes of sign. For negative values of  $\alpha$ , see Fig. 4, the difference  $\sigma_1 - \sigma_2$  is obviously a non-monotonic function of the curvature exhibiting regions of unbroken charge symmetry, corresponding to  $\sigma_1 = \sigma_2$ , as well as regions of broken charge symmetry with  $\sigma_1 \neq \sigma_2$ , with the difference between the two surface charge densities varying from positive values to negative values on increasing the curvature. In fact this behavior can be seen clearly also in Fig. 3 where it corresponds to an curvature cut through the three lines of charge symmetry for a fixed  $(\alpha, \chi)$  combination in the phase diagram. Clearly for a sufficiently negative  $\alpha$ , *e.g.* for  $(\alpha, \chi)$  combination  $(-20, 5)$ , the difference between the inner and outer charge density,  $\sigma_1 - \sigma_2$  ceases to change sign within both the theories, but their non-monotonic behavior is still retained. The two thus represent separate features of the charging state of the curved bilayer. The behavior for the positive values of  $\alpha$ , see Fig. 5, differs significantly. For a variety of  $(\alpha, \chi)$  cuts through the phase diagram we detect here no changes in sign for the difference between the inner and outer charge density, but we do see remarkable

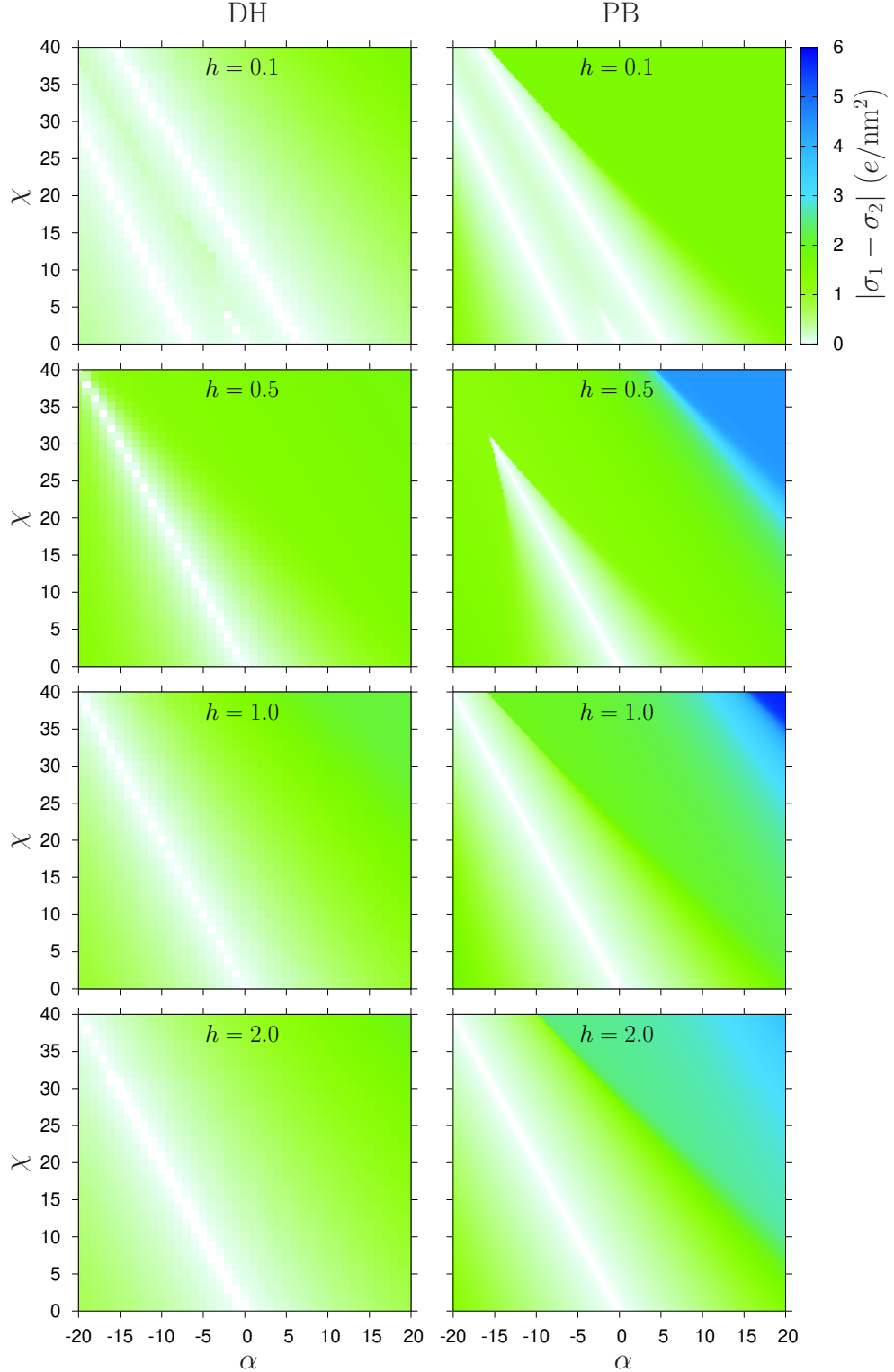


FIG. 3. The variation of the absolute value of the difference of the charge densities at the two surfaces of the bilayer,  $|\sigma_1 - \sigma_2|$ , expressed in the units of  $e/nm^2$ , as function of  $\alpha$  and  $\chi$  for four different choices of the curvature  $h = 0.1, 0.5, 1.0, 2.0$  obtained within the DH theory (left panels) as well as within the PB theory (right panels). The white regions in each plot correspond to symmetric states with  $\sigma_1 = \sigma_2$  whereas the colored regions correspond to asymmetric states with  $\sigma_1 \neq \sigma_2$ .

non-monotonicity in its dependence on curvature with very clear-cut differences between the PB and DH results. Nevertheless,  $\sigma_1 - \sigma_2$  seems to increase for small curvature, reaching a local maximum, then dropping and increasing again but less steeply for larger curvatures. As for the range of curvatures that we display on Fig. 5, one also needs to consider the inherent limitations of the continuum assumptions which form the basis of the present calculations and the curvature should not be extended to arbitrary large values.

The curvature dependence of the difference in surface charge density between the inner and outer leaflet,  $\sigma_1 - \sigma_2$ , implies the existence of a *dipolar moment* in the direction of the normal of the bilayer, and therefore also the *existence of flexoelectricity*, but with a variable magnitude and sign. Flexoelectricity is a general mechano-electric phenomenon in liquid crystal physics [38] but has important consequences specifically in the context of lipid membranes as argued by Petrov [59, 60]. In the small deformation continuum limit regime, the induced flexoelectric polarization is proportional to the membrane curvature and a simple Langmuir isotherm based charge regulation model was invoked as a possible microscopic origin for the flexoelectric coefficient in the seminal work of Derzhansky and coworkers [39]. Our calculations generalize this approach and uncover

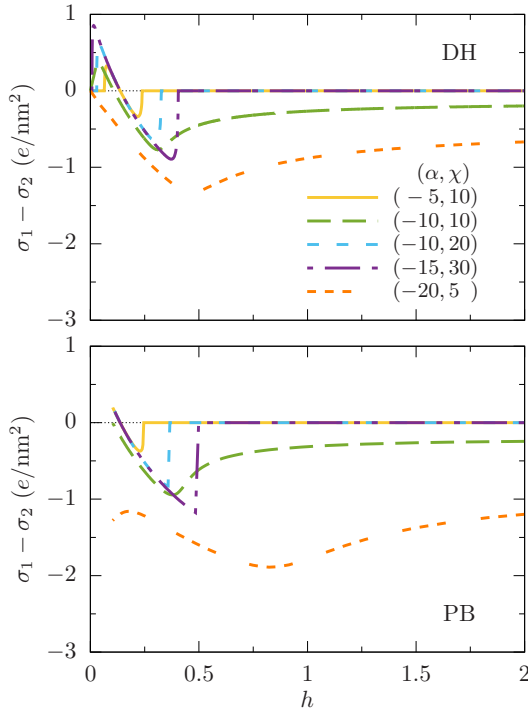


FIG. 4. Variations of the differences in the charge densities,  $\sigma_1 - \sigma_2$ , expressed in the units of  $e/\text{nm}^2$ , as function of the curvature  $h$  for different combinations of the  $\alpha$  and the  $\chi$  parameters with  $\alpha$  being always negative (corresponding to a favorable adsorption free energy for the protons onto the vesicle surfaces). Within both the theories (DH theory in the upper panel and PB theory in the lower panel) the results are qualitatively the same, i.e., for  $\alpha$  and  $\chi$  satisfying the relation  $\chi = -2\alpha$ , the charge density difference  $\sigma_1 - \sigma_2$  shows a discontinuous transition from a finite non-zero value to zero as the curvature  $h$  is increased. However, for other combinations of the  $\alpha$  and  $\chi$  parameters, the charge density difference  $\sigma_1 - \sigma_2$  do not show any such discontinuous transition.

new phenomena corresponding to symmetry breaking in charge regulated systems [21]. Clearly, the region of a simple proportionality between the bilayer polarization and curvature is limited and depends crucially on the charge regulation parameters.

For  $\alpha > 0$ , Fig. 5, the difference  $\sigma_1 - \sigma_2$  does not in general change sign, but remains nevertheless non-monotonic so that the system remains in a broken charge symmetry state for all indicated values of the charge regulation parameters  $\alpha$  and  $\chi$ . The calculations seem to indicate two separate regions of approximately linear flexoelectricity, but with flexoelectric coefficients of different magnitude: one at small curvatures (below  $h \simeq 0.5$  for PB calculations and  $h \simeq 0.1$  for DH calculations) and another one at larger curvatures (above  $h \simeq 0.75$  for PB calculations and  $h \simeq 0.2$  for DH calculations), until finally  $\sigma_1 - \sigma_2$  varies only weakly with curvature. For  $\alpha \ll 0$ , Fig. 4, the situation seems more complicated and also the differences between the PB and DH calculations more evident. There appears a linear flexoelectric regime at very small curvatures that changes sign for larger curvatures (evident for e.g.  $\alpha, \chi = -20, 5$  or  $-10, 10$  case for PB and DH calculations, Fig. 4). As  $\chi$  is increased the linear flexoelectric regime for small curvatures is eventually cut short for large enough curvatures and the system fully restores its charge symmetry with vanishing flexoelectricity (evident for e.g.  $\alpha, \chi = -15, 30$  case for PB and DH calculations, Fig. 4). Since the PB calculation cannot probe the regime of very small curvature because of numerical problems we

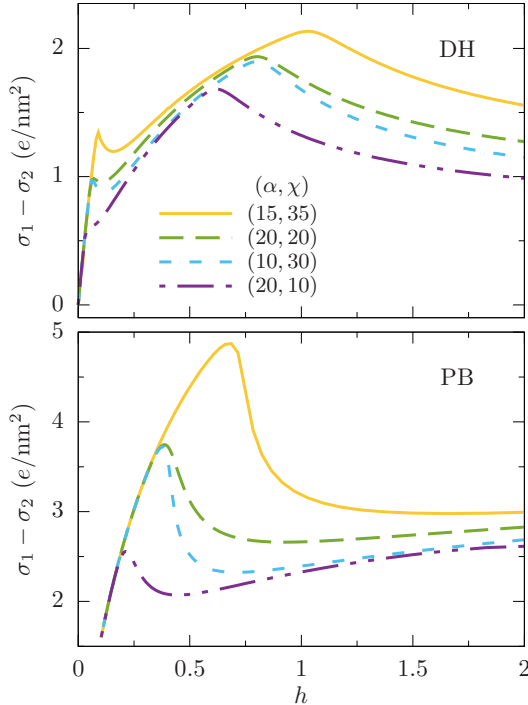


FIG. 5. Variations of the differences in the charge densities,  $\sigma_1 - \sigma_2$ , expressed in the units of  $e/\text{nm}^2$ , as function of the curvature  $h$  for different combinations of the  $\alpha$  and the  $\chi$  parameters with  $\alpha$  being always positive. Within both the theories (DH theory in the upper panel and PB theory in the lower panel), one observes a similar trend, i.e., the charge density difference  $\sigma_1 - \sigma_2$  increases initially to reach a maximum, then goes down and increases again following a minimum. Within the range of  $h$  considered here, the results obtained within the DH theory shows the occurrence of a second maximum as well.

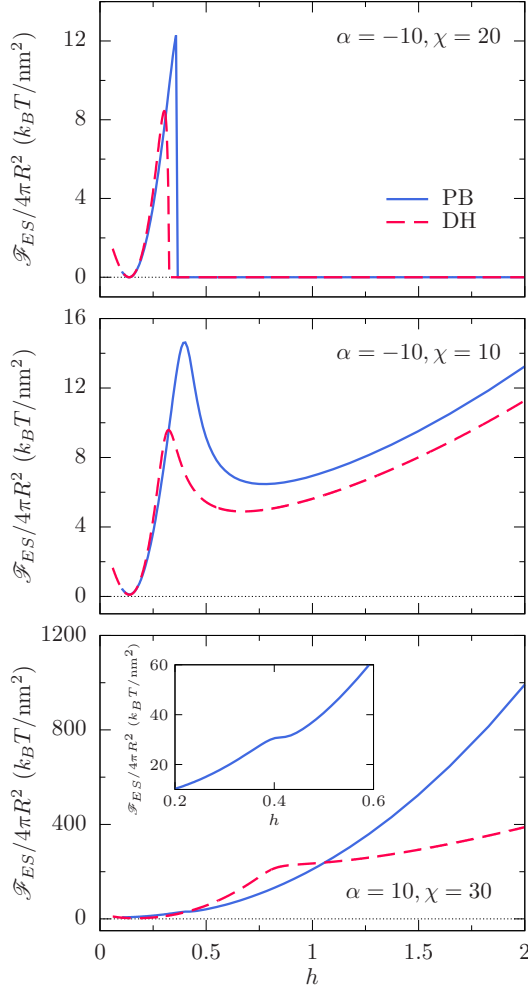


FIG. 6. Variations of the electrostatic part  $\mathcal{F}_{ES}$  of the free energy per unit inner surface area  $4\pi R^2$ , expressed in the units of  $k_B T/\text{nm}^2$ , as function of the curvature  $h$  for different  $\alpha$  and  $\chi$  values. For a given  $(\alpha, \chi)$  parameter combination, the results obtained within the linearized PB or DH theory are plotted using red dashed lines whereas those obtained using the nonlinear PB theory are plotted using solid blue lines. Contrary to the widely used approximation,  $\mathcal{F}_{ES}/4\pi R^2$  does not in general show a  $h^2$ -dependence. While it does mostly vary  $\propto h^2$  or  $\propto (h - h_0)^2$  for  $\alpha > 0$ , the situation is richer for  $\alpha < 0$  involving the presence of multiple minima and even vanishing contribution corresponding to charge-neutral surfaces for sufficiently large curvature values.

can rely only on the DH results that show a vanishing flexoelectricity also for very small curvatures at not too large  $\alpha < 0$  and  $\chi > 0$ . The non-linear features of flexoelectricity just described are pertinent to the charge regulation model which takes into account certain salient features of the phospholipid protonation/deprotonation reactions at the membrane-electrolyte solution boundary. They do not appear in fixed charge models of membrane electrostatics. Furthermore it is clear that the property of flexoelectricity depends crucially on the phospholipid dissociation properties as well as the solution conditions, far from being a universal property of the membrane composition.

We finally examine the hypothesis that the electrostatic effects in membrane can be reduced to a

renormalized spontaneous curvature and renormalized bending rigidity, standardly invoked in the context of electrostatic interactions in phospholipid membranes [35, 37, 40]. In Fig. 6 we plot the curvature dependence of the equilibrium electrostatic surface free energy density as obtained from the linearized DH or fully non-linear PB theory. If indeed the electrostatic effects could be reduced solely to renormalized values of the bending rigidity and spontaneous curvature, then the curvature dependence of the equilibrium electrostatic surface free energy density should show a parabolic dependence centered at the spontaneous curvature. What we observe in Fig. 6 corroborates this expectations but only for positive values of  $\alpha$ . In general, and in particular for negative values of  $\alpha$ , however, the curvature dependence exhibits a behavior quite different from these expectations. In this case one observes, see Fig. 6, multiple curvature minima and in some cases a vanishing value of the electrostatic free energy as both surfaces become completely neutralized. The paradigm of renormalized spontaneous curvature and renormalized bending rigidity has thus only a limited validity and its range of applicability depends again crucially on the phospholipid dissociation properties and solution conditions. The membrane composition, affecting the two charge regulation parameters, indeed plays a role in the curvature properties but so do the bathing solution conditions that collectively determine the nature and magnitude of electrostatic effects.

#### IV. DISCUSSION

There are of course a plethora of works based on molecular and coarse grained simulations of lipid bilayers and their interactions [61–63] but none of these studies exhaustively explored the contribution of electrostatic interactions to the charge states of dissociable lipid headgroups [8]. Even in the most accurate parametrization of the lipid molecular force fields that take into account the dissociation state of the lipid headgroup through the partial charges, the charge regulation, *i.e.*, the dependence of the dissociation state on the local bathing solution conditions, is usually not considered [64]. To include the effects discussed in our paper one would need to implement the charge dissociation reactions explicitly into the simulation scheme along the lines of recent advances in the simulation techniques for reaction ensembles [65, 66]. Inclusion of the explicit charge regulation model into the detailed mean-field electrostatic theory applied to a curved phospholipid bilayer membrane allowed us to uncover and analyse several effects that have heretofore remained outside the electrostatic renormalization of the membrane mechanical properties [37].

The first effect depending on the detailed charge regulation mechanism is the charge symmetry breaking, leading to unequal charges of the inner and outer phospholipid membrane surface even if - and this is important - they be chemically identical, *i.e.* described by the same free energy parameters. This effect was first observed in the case of membranes interacting across an electrolyte solution [21, 22], however, the charge symmetry breaking for a curved bilayer differs from this case since the two charged surfaces in a membrane interact across a simple dielectric, and charge symmetry breaking is in some sense inverse to the case of interacting membranes. In the most drastic case the charge symmetry broken state can be characterized by one of the monolayers near neutral and only one charged, or both charged but with charges of opposite sign.

The second important effect is the existence non-linear flexoelectricity, with flexoelectricity itself being well known and even explained by a type of charge regulation mechanism for membranes [39]. Nevertheless, including more detailed charge regulation description and full mean-field electrostatic

theory indicates that the flexoelectric constitutive relation is in general not linear and in addition its form depends crucially on the charge regulation parameters. Only certain intervals of dissociation parameters would correspond coarsely to a linear flexoelectric constitutive relation, with dipolar moment proportional to the curvature. In general, however, the proportionality is non-linear or there might actually be no flexoelectricity for sufficiently large curvatures.

The last important modification in our analysis of the charge regulation effects is the dependence of the free energy on the curvature. As stated before, the prevailing paradigm is to see the electrostatic effects as commonly renormalizing the elasto-mechanical properties of the membrane, such as surface tension, curvature and bending rigidity (for a recent description see Ref. [37]). Our results indicate that this is not the complete story and that the free energy of a charge-regulated phospholipid membrane exhibits a much richer variety of curvature dependence. Only for a limited interval of the phospholipid dissociation parameters does one indeed observe a clear quadratic dependence on curvature that would be consistent with the electrostatic renormalization of the membrane elasto-mechanics.

The bilayer membrane asymmetry need not necessarily involve the obviously asymmetric protein distribution in biological membranes. It can also exhibit differences in lipid composition between the two leaflets [67] or be a consequence of different solution conditions across the separating membrane [68]. Based on our calculations we can state that even without *any* compositional asymmetry, or *any* solution asymmetry, the phospholipid dissociation coupled to electrostatic interactions and curvature would itself contribute an essential charge asymmetry to the otherwise completely symmetric membrane properties.

Experimentally, the very same model that we used above to describe the charge regulated membrane electrostatics was used to elucidate the liquid-liquid ( $L_\alpha \rightarrow L_{\alpha'}$ ) phase transition observed in osmotic pressure measurements of certain charged amphiphilic membranes [41]. The phenomenon of charge symmetry breaking, that can induce attractions between chemically identical membranes, was argued to induce an attractive disjoining pressure in plant thylakoid membranes and photosynthetic membranes of a family of cyanobacteria [22]. We are thus confident that the charge regulation effects coupled to membrane curvature are real and could be detected in solutions of varying acidity and salt activity. While there is no lack in experiments probing the effects of pH on membrane properties of giant unilamellar vesicle such as a pH change induced vesicle migration and global deformation [69], vesicle polarization coupled to phase-separated membrane domains [70] and the effect of localized pH heterogeneities on membrane deformations [71], a systematic quantitative comparison between expected pH-induced effects and observed membrane response is lacking. One of the reasons for this is that the pH-curvature coupling is complicated and non-linear, as we argued and demonstrated above. The phenomenology of this coupling presented in this work should help to elucidate the details of the pH effects and the role played by the dissociation mechanism in phospholipid membranes.

## V. ACKNOWLEDGMENTS

RP and PK acknowledge funding from the Key Project No. 12034019 of the National Natural Science Foundation of China and the 1000-Talents Program of the Chinese Foreign Experts Bureau and the School of Physics, University of Chinese Academy of Sciences.

## Appendix A: The total free energy density

The total free energy density of our charge-regulated lipid bilayers system is the sum of the electrostatic free energy, the charge regulation free energy, and the curvature-lipid density coupling free energy:

$$\frac{\mathcal{F}_{tot}(n_1, n_2; \eta_1, \eta_2; h)}{4\pi R^2} = \frac{\mathcal{F}_{ES}(n_1, n_2; \eta_1, \eta_2; h)}{4\pi R^2} + \frac{\mathcal{F}_{HE}(n_1, n_2; h)}{4\pi R^2} + \frac{\mathcal{F}_{CR}(\eta_1; h) + \mathcal{F}_{CR}(\eta_2; h)}{4\pi R^2}. \quad (A1)$$

The electrostatic free energy per area was obtained as a function of the radius of curvature  $R$  to inverse quadratic order in Ref. [40] and can be rewritten as

$$\begin{aligned}
\frac{\mathcal{F}_{ES}(n_1, n_2; \eta_1, \eta_2)}{4\pi R^2} = & \frac{2\pi\ell_B k_B T}{\kappa_D} \left[ \left( \frac{1}{2\mu + \kappa_D w} \right) \left( (\mu + \kappa_D w) ((2\eta_1 - 1)^2 n_1^2 + (2\eta_2 - 1)^2 n_2^2) \right. \right. \\
& + 2\mu n_1 n_2 (2\eta_1 - 1)(2\eta_2 - 1) \Big) + \left( \frac{\kappa_D w}{2\mu + \kappa_D w} \right) \left( \frac{1}{\kappa_D R} \right) \left( -(\mu - 1)(2\eta_1 - 1)^2 n_1^2 \right. \\
& + (3\mu + 2\kappa_D w - 1)(2\eta_2 - 1)^2 n_2^2 + 2\mu n_1 n_2 (2\eta_1 - 1)(2\eta_2 - 1) \Big) \\
& + \frac{\kappa_D w}{(2\mu + \kappa_D w)^2} \frac{1}{(\kappa_D R)^2} \left( (\mu - 1) \{ \kappa_D w(\mu - 1) - \mu \} (2\eta_1 - 1)^2 n_1^2 \right. \\
& + \left. \left. \left. \left\{ (\kappa_D w)^3 + (\kappa_D w)^2 (4\mu - 1) + (\kappa_D w) (5\mu^2 - 4\mu + 1) - \mu(\mu - 1) \right\} (2\eta_2 - 1)^2 n_2^2 \right. \right. \\
& \left. \left. - 2n_1 n_2 \mu(\mu - 1)(1 + \kappa_D w)(2\eta_1 - 1)(2\eta_2 - 1) \right) \right]. \tag{A2}
\end{aligned}$$

Using this, within the Debye-Hückel (DH) theory the total free energy density in Eq. (A1) is given explicitly by

$$\begin{aligned}
\frac{\mathcal{F}_{tot}(n_1, n_2; \eta_1, \eta_2; h)}{4\pi R^2} = & \frac{2\pi\ell_B k_B T}{\kappa_D} \left[ \left( \frac{1}{2\mu + \kappa_D w} \right) \left( (\mu + \kappa_D w) \left( (2\eta_1 - 1)^2 n_1^2 + (2\eta_2 - 1)^2 n_2^2 \right) \right. \right. \\
& + 2\mu n_1 n_2 (2\eta_1 - 1)(2\eta_2 - 1) \Big) + \left( \frac{h\kappa_D w}{2\mu + \kappa_D w} \right) \left( -(\mu - 1)(2\eta_1 - 1)^2 n_1^2 \right. \\
& \left. \left. + (3\mu + 2\kappa_D w - 1)(2\eta_2 - 1)^2 n_2^2 + 2\mu n_1 n_2 (2\eta_1 - 1)(2\eta_2 - 1) \right) \right. \\
& + \frac{h^2 \kappa_D w}{(2\mu + \kappa_D w)^2} \left( (\mu - 1) \{ (\kappa_D w)(\mu - 1) - \mu \} (2\eta_1 - 1)^2 n_1^2 \right. \\
& \left. + \left\{ (\kappa_D w)^3 + (\kappa_D w)^2 (4\mu - 1) + \kappa_D w (5\mu^2 - 4\mu + 1) - \mu(\mu - 1) \right\} (2\eta_2 - 1)^2 n_2^2 \right. \\
& \left. - 2n_1 n_2 \mu(\mu - 1)(1 + \kappa_D w)(2\eta_1 - 1)(2\eta_2 - 1) \right) \Big] + \left( 1 + \frac{h\kappa_D w}{2} \right)^2 \\
& \times \left[ \frac{k_s}{2} \left( \frac{n_1}{n_0} - 1 - \frac{4h\kappa_D w}{2 + h\kappa_D w} \right)^2 + \frac{k_s}{2} \left( \frac{n_2}{n_0} - 1 + \frac{4h\kappa_D w}{2 + h\kappa_D w} \right)^2 + \frac{8k_b (h\kappa_D)^2}{(2 + h\kappa_D w)^2} \right] \\
& + n_0 k_B T \left( -\alpha \eta_1 - \frac{\chi}{2} \eta_1^2 + \eta_1 \ln \eta_1 + (1 - \eta_1) \ln(1 - \eta_1) \right) \\
& + n_0 k_B T (1 + h\kappa_D w)^2 \left( -\alpha \eta_2 - \frac{\chi}{2} \eta_2^2 + \eta_2 \ln \eta_2 + (1 - \eta_2) \ln(1 - \eta_2) \right). \quad (\text{A3})
\end{aligned}$$

The total free energy density Eq. (A3) needs to be minimized with respect to the charge fractions  $\eta_{1,2}$  and the lipid densities  $n_{1,2}$ .

## Appendix B: Limiting form of the free energy, very large $k_s$

In this case the total free energy density in the DH case can be derived in the simplified form of

$$\begin{aligned}
\frac{\mathcal{F}_{tot}(\eta_1, \eta_2; h)}{4\pi R^2} = & \frac{2\pi n_0^2 \ell_B k_B T}{\kappa_D} \left[ \left( \frac{1}{2\mu + \kappa_D w} \right) \left\{ (\mu + \kappa_D w) \left( (2\eta_1 - 1)^2 \left( 1 + \frac{4h\kappa_D w}{2 + h\kappa_D w} \right)^2 \right. \right. \right. \\
& + (2\eta_2 - 1)^2 \left( 1 - \frac{4h\kappa_D w}{2 + h\kappa_D w} \right)^2 \left. \right) + 2\mu(2\eta_1 - 1)(2\eta_2 - 1) \left( 1 - \frac{(4h\kappa_D w)^2}{(2 + h\kappa_D w)^2} \right) \left. \right\} \\
& + \left( \frac{h\kappa_D w}{2\mu + \kappa_D w} \right) \left\{ -(\mu - 1)(2\eta_1 - 1)^2 \left( 1 + \frac{4h\kappa_D w}{2 + h\kappa_D w} \right)^2 + (3\mu + 2\kappa_D w - 1) \right. \\
& \times (2\eta_2 - 1)^2 \left( 1 - \frac{4h\kappa_D w}{2 + h\kappa_D w} \right)^2 + 2\mu(2\eta_1 - 1)(2\eta_2 - 1) \left( 1 - \frac{(4h\kappa_D w)^2}{(2 + h\kappa_D w)^2} \right) \left. \right\} \\
& + \frac{h^2 \kappa_D w}{(2\mu + \kappa_D w)^2} \left\{ (\mu - 1) \{ (\kappa_D w)(\mu - 1) - \mu \} (2\eta_1 - 1)^2 \left( 1 + \frac{4h\kappa_D w}{2 + h\kappa_D w} \right)^2 \right. \\
& + \{ (\kappa_D w)^3 + (\kappa_D w)^2 (4\mu - 1) + (\kappa_D w)(5\mu^2 - 4\mu + 1) - \mu(\mu - 1) \} (2\eta_2 - 1)^2 \\
& \times \left( 1 - \frac{4h\kappa_D w}{2 + h\kappa_D w} \right)^2 - 2\mu(\mu - 1)(1 + \kappa_D w)(2\eta_1 - 1)(2\eta_2 - 1) \left( 1 - \frac{(4h\kappa_D w)^2}{(2 + h\kappa_D w)^2} \right) \left. \right\} \\
& + \frac{8k_b(h\kappa_D)^2}{(2 + h\kappa_D w)^2} + n_0 k_B T \left( -\alpha\eta_1 - \frac{\chi}{2}\eta_1^2 + \eta_1 \ln \eta_1 + (1 - \eta_1) \ln(1 - \eta_1) \right) \\
& + n_0 k_B T (1 + h\kappa_D w)^2 \left( -\alpha\eta_2 - \frac{\chi}{2}\eta_2^2 + \eta_2 \ln \eta_2 + (1 - \eta_2) \ln(1 - \eta_2) \right). \quad (B1)
\end{aligned}$$

Clearly, the total free energy density Eq. (B1) has reduced the number of variables to two.

- 
- [1] T. Markovich, D. Andelman, and R. Podgornik, in *Handbook of Lipid Membranes*, edited by C. R. Safinya and J. O. Raedler (Taylor & Francis, 2021).
- [2] G. V. Bossa, K. Bohinc, and S. May, in *Handbook of Lipid Membranes*, edited by C. R. Safinya and J. O. Raedler (Taylor & Francis, 2021).
- [3] Y. Hong and D. G. Brown, *Langmuir* **24**, 5003 (2008).
- [4] K. K. Ewert, P. Scodeller, L. Simón-Gracia, V. M. Steffes, E. A. Wonder, T. Teesalu, and C. R. Safinya, *Pharmaceutics* **13**, 1365 (2021).
- [5] G. Cevc, *Biochim. Biophys. Acta* **1031**, 311 (1990).
- [6] M. J. Mulligan, K. E. Lyke, N. Kitchin, J. Absalon, A. Gurtman, S. Lockhart, K. Neuzil, V. Raabe, R. Bailey, K. A. Swanson, P. Li, K. Koury, W. Kalina, D. Cooper, C. Fontes-Garfias, P.-Y. Shi, O. Türeci, K. R. Tompkins, E. E. Walsh, R. Frenck, A. R. Falsey, P. R. Dormitzer, W. C. Gruber, U. Şahin, and K. U. Jansen, *Nature* **586**, 589 (2020).
- [7] L. R. Baden, H. M. El Sahly, B. Essink, K. Kotloff, S. Frey, R. Novak, D. Diemert, S. A. Spector, N. Rouphael, C. B. Creech, J. McGettigan, S. Khetan, N. Segall, J. Solis, A. Brosz, C. Fierro, H. Schwartz, K. Neuzil, L. Corey, P. Gilbert, H. Janes, D. Follmann, M. Marovich, J. Mascola,

- L. Polakowski, J. Ledgerwood, B. S. Graham, H. Bennett, R. Pajon, C. Knightly, B. Leav, W. Deng, H. Zhou, S. Han, M. Ivarsson, J. Miller, and T. Zaks, *N. Engl. J. Med.* **384**, 403 (2021).
- [8] M. Schlich, R. Palomba, G. Costabile, S. Mizrahy, M. Pannuzzo, D. Peer, and P. Decuzzi, *Bioeng. Transl. Med.* **6**, e10213 (2021).
- [9] C. Holm, P. Kékicheff, and R. Podgornik, eds., *Electrostatic Effects in Soft Matter and Biophysics*, 1st ed. (Kluwer, Dordrecht, 2001).
- [10] M. Borkovec, B. Jönsson, and G. J. M. Koper, in *Surface and Colloid Science. Surface and Colloid Science*, edited by E. Matijević (Springer, 2001).
- [11] M. Lund and B. Jönsson, *Biochemistry* **44**, 5722 (2005).
- [12] F. L. Barroso da Silva and B. Jönsson, *Soft Matter* **5**, 2862 (2009).
- [13] F. L. Barroso da Silva and L. G. Dias, *Biophys. Rev.* **9**, 699 (2017).
- [14] Y. Avni, T. Markovich, R. Podgornik, and D. Andelman, *Soft Matter* **14**, 6058 (2018).
- [15] R. Podgornik, D. Harries, J. Derouchey, H. Strey, and V. A. Parsegian, in *Gene and Cell Therapy: Therapeutic Mechanisms and Strategies*, edited by N. S. Templeton (CRC Press, 2008) pp. 443–484.
- [16] B. W. Ninham and V. A. Parsegian, *J. Theor. Biol.* **31**, 405 (1971).
- [17] R. Podgornik, *J. Chem. Phys.* **149**, 104701 (2018).
- [18] R. J. Nap, A. L. Božič, I. Szleifer, and R. Podgornik, *Biophysical Journal* **107**, 1970 (2014).
- [19] M. I. Angelova, A.-F. Bitbol, M. Seigneuret, G. Staneva, A. Kodama, Y. Sakuma, T. Kawakatsu, M. Imai, and N. Puff, *Biochim. Biophys. Acta, Biomembr.* **1860**, 2042 (2018).
- [20] M. Jayaraman, S. M. Ansell, B. L. Mui, Y. K. Tam, J. Chen, X. Du, D. Butler, L. Eltepu, S. Matsuda, J. K. Narayananair, K. G. Rajeev, I. M. Hafez, A. Akinc, M. A. Maier, M. A. Tracy, P. R. Cullis, T. D. Madden, M. Manoharan, and M. J. Hope, *Angew. Chem., Int. Ed.* **51**, 8529 (2012).
- [21] A. Majee, M. Bier, and R. Podgornik, *Soft Matter* **14**, 985 (2018).
- [22] A. Majee, M. Bier, R. Blossey, and R. Podgornik, *Phys. Rev. E* **100**, 050601 (2019).
- [23] A. Majee, M. Bier, R. Blossey, and R. Podgornik, *Phys. Rev. Research* **2**, 043417 (2020).
- [24] V. V. Galassi and N. Wilke, *Membranes* **11**, 478 (2021).
- [25] S. Pöyry and I. Vattulainen, *Biochim. Biophys. Acta, Biomembr.* **1858**, 2322 (2016).
- [26] D. Marsh, *Handbook of Lipid Bilayers*, 2nd ed. (CRC Press, 2013).
- [27] M. H. M. Olsson, C. R. Søndergaard, M. Rostkowski, and J. H. Jensen, *J. Chem. Theory Comput.* **7**, 525 (2011).
- [28] G. Cevc, in *Encyclopedia of Biophysics*, edited by G. C. K. Roberts and A. Watts (Springer Berlin Heidelberg, 2018).
- [29] R. Leventis and J. R. Silvius, *Biochim. Biophys. Acta, Biomembr.* **1023**, 124 (1990).
- [30] J. R. Casey, S. Grinstein, and J. Orlowski, *Nat. Rev. Mol. Cell Biol.* **11**, 50 (2010).
- [31] N. Ben-Dov and R. Korenstein, *PLoS ONE* **7**, e35204 (2012).
- [32] M. Lund and B. Jönsson, *Q. Rev. Biophys.* **46**, 265 (2013).
- [33] L. Javidpour, A. Božič, A. Naji, and R. Podgornik, *Soft Matter* **17**, 4296 (2021).
- [34] E. Tanguy, N. Kassas, and N. Vitale, *Biomolecules* **8**, 20 (2018).
- [35] D. Andelman, in *Handbook of Biological Physics: Structure and Dynamics of Membranes*, edited by R. Lipowsky and E. Sackmann (Elsevier, 1995).
- [36] A. Fogden and B. Ninham, *Adv. Colloid Interface Sci.* **83**, 85 (1999).

- [37] H. A. Faizi, S. L. Frey, J. Steinkühler, R. Dimova, and P. M. Vlahovska, *Soft Matter* **15**, 6006 (2019).
- [38] A. G. Petrov, *The Lyotropic State of Matter: Molecular Physics and Living Matter Physics*, 1st ed. (CRC Press, New York, 1999).
- [39] K. Hristova, I. Bivas, A. G. Petrov, and A. Derzhanski, *Mol. Cryst. Liq. Cryst.* **200**, 71 (1991).
- [40] H. R. Shojaei, A. L. Božić, M. Murugappan, and R. Podgornik, *Phys. Rev. E* **93**, 052415 (2016).
- [41] D. Harries, R. Podgornik, V. A. Parsegian, E. Mar-Or, and D. Andelman, *J. Chem. Phys.* **124**, 224702 (2006).
- [42] L. Koopal, W. Tan, and M. Avena, *Adv. Colloid Interface Sci.* **280**, 102138 (2020).
- [43] N. Adžić and R. Podgornik, *Eur. Phys. J. E* **37**, 49 (2014).
- [44] I. Teraoka, *Polymer solutions: An Introduction to Physical Properties* (John Wiley & Sons, Inc., New York, 2002).
- [45] Y. Avni, R. Podgornik, and D. Andelman, *J. Chem. Phys.* **153**, 024901 (2020).
- [46] E. J. Verwey and J. T. G. Overbeek, *Theory of the stability of Lyophobic Colloids* (Elsevier, Amsterdam, 1948).
- [47] A. Majee, M. Bier, and S. Dietrich, *J. Chem. Phys.* **145**, 064707 (2016).
- [48] M. Winterhalter and W. Helfrich, *J. Phys. Chem.* **92**, 6865 (1988).
- [49] D. J. Mitchell and B. W. Ninham, *Langmuir* **5**, 1121 (1989).
- [50] H. Lekkerkerker, *Physica A* **167**, 384 (1990).
- [51] B. Duplantier, R. E. Goldstein, V. Romero-Rochin, and A. I. Pesci, *Phys. Rev. Lett.* **65**, 508 (1990).
- [52] J. L. Harden, C. Marques, J. F. Joanny, and D. Andelman, *Langmuir* **8**, 1170 (1992).
- [53] S. Svetina and B. Žekš, *Adv. Colloid Interface Sci.* **208**, 189 (2014).
- [54] X. Bian, S. Litvinov, and P. Koumoutsakos, *Computer Methods in Applied Mechanics and Engineering* **359**, 112758 (2020).
- [55] C. R. Safinya and J. Radler, *Handbook of Lipid Membranes: Molecular, Functional, and Materials Aspects* (CRC Press, 2021).
- [56] A.-F. Bitbol, L. Peliti, and J.-B. Fournier, *Eur. Phys. J. E* **34**, 53 (2011).
- [57] U. Seifert and S. A. Langer, *Europhys. Lett.* **23**, 71 (1993).
- [58] Y. Avni, D. Andelman, and R. Podgornik, *Curr. Opin. Electrochem.* **13**, 70 (2019).
- [59] A. G. Petrov, *Biochim. Biophys. Acta, Biomembr.* **1561**, 1 (2002).
- [60] A. G. Petrov, *Anal. Chim. Acta* **568**, 70 (2006).
- [61] S. E. Feller, *Curr. Opin. Colloid Interface Sci.* **5**, 217 (2000).
- [62] Z.-J. Wang and M. Deserno, *J. Phys. Chem. B* **114**, 11207 (2010).
- [63] S. Y. Joshi and S. A. Deshmukh, *Mol. Simul.* **47**, 786 (2021).
- [64] Y. Yu, A. Krämer, R. M. Venable, B. R. Brooks, J. B. Klauda, and R. W. Pastor, *J. Chem. Theory Comput.* **17**, 1581 (2021).
- [65] J. Landsgesell, P. Hebbeker, O. Rud, R. Lunkad, P. Košovan, and C. Holm, *Macromolecules* **53**, 3007 (2020).
- [66] T. Cerk, J. Yuan, and E. Luijten, arXiv (2021), [arXiv:2109.07527 \[cond-mat.soft\]](https://arxiv.org/abs/2109.07527).
- [67] H. I. Ingólfsson, M. N. Melo, F. J. van Eerden, C. Arnarez, C. A. Lopez, T. A. Wassenaar, X. Periole, A. H. de Vries, D. P. Tieleman, and S. J. Marrink, *J. Am. Chem. Soc.* **136**, 14554 (2014).
- [68] M. Karimi, J. Steinkühler, D. Roy, R. Dasgupta, R. Lipowsky, and R. Dimova, *Nano Lett.* **18**, 7816 (2018).

- [69] A. Kodama, Y. Sakuma, M. Imai, Y. Oya, T. Kawakatsu, N. Puff, and M. I. Angelova, *Soft Matter* **12**, 2877 (2016).
- [70] G. Staneva, N. Puff, M. Seigneuret, H. Conjeaud, and M. I. Angelova, *Langmuir* **28**, 16327 (2012).
- [71] N. Khalifat, J.-B. Fournier, M. I. Angelova, and N. Puff, *Biochim. Biophys. Acta, Biomembr.* **1808**, 2724 (2011).